

---

# RegionViT: Regional-to-Local Attention for Vision Transformers

---

Chun-Fu (Richard) Chen, Rameswar Panda, Quanfu Fan  
MIT-IBM Watson AI Lab  
chenrich@us.ibm.com, rpanda@ibm.com, qfan@us.ibm.com

## Abstract

Vision transformer (ViT) has recently showed its strong capability in achieving comparable results to convolutional neural networks (CNNs) on image classification. However, vanilla ViT simply inherits the same architecture from the natural language processing directly, which is often not optimized for vision applications. Motivated by this, in this paper, we propose a new architecture that adopts the pyramid structure and employ a novel regional-to-local attention rather than global self-attention in vision transformers. More specifically, our model first generates regional tokens and local tokens from an image with different patch sizes, where each regional token is associated with a set of local tokens based on the spatial location. The regional-to-local attention includes two steps: first, the regional self-attention extract global information among all regional tokens and then the local self-attention exchanges the information among one regional token and the associated local tokens via self-attention. Therefore, even though local self-attention confines the scope in a local region but it can still receive global information. Extensive experiments on three vision tasks, including image classification, object detection and action recognition, show that our approach outperforms or is on par with state-of-the-art ViT variants including many concurrent works. Our source codes and models will be publicly available.

## 1 Introduction

Transformers [42] based on self-attention come naturally with the ability to learn long-range dependencies in sequential data. As important as it is to language modeling [12], such ability is also highly desired for many vision tasks where contextual modeling plays a significant role. For this reason, self-attention and transformers have been receiving an increasing attention in the vision community [1, 36, 56, 34, 2, 21, 35, 44]. Especially, the recently proposed Vision Transformers (ViT) [13] demonstrates comparable image classification results against the firmly established and prevalent CNNs [18, 39, 4] in computer vision, albeit relying on a huge amount of training data. It has since then led to an explosion of interest [48, 43, 19, 54, 27, 15, 30, 7, 50, 6] in further investigating its potential for a wide variety of vision applications.

The ViT inherits the entire architecture from the vanilla transformer [42], which is designed for natural language processing tasks, and some of those designs thus may not meet the needs of vision tasks. For example, the transformer has a isotropic network structure with a fixed number of tokens and unchanged embedding size, which loses the capability to model the context with different scales and allocates computations at different scales. As opposed to this, a majority of CNNs adopt a popular pyramid architecture to compute multi-scale features efficiently. In light of this, recent vision transformers such as PVT [43] and PiT [19] follow a similar pyramid structure in CNNs, showing improvement on both computation and memory efficiency as well as on model accuracy. Another critical bottleneck of the transformer is that the self-attention module has a quadratic cost in memory and computation with regard to the sequence length (i.e., the number of tokens). This issue is

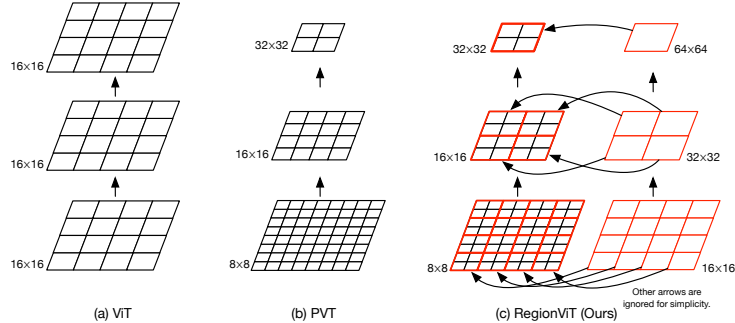


Figure 1: **Regional-to-Local Attention for Vision Transformers.** (a) The vanilla ViT [13] uses a fixed patch size through the whole network while (b) PVT [43] adopts a pyramid structure to gradually enlarge the patch size (i.e. reduce the spatial resolution) in the network. Both ViT and PVT attend to all the tokens at each layer, which are compute- and memory-intensive. (c) Our proposed approach combines a pyramid structure with an efficient regional-to-local (R2L) attention mechanism to reduce computation and memory usage in self-attention. Our approach divides the input image into two groups of tokens, regional tokens of large patch size (red) and local ones of small patch size (black), processing them separately by a transformer. The two types of tokens communicate efficiently through local attention, which jointly attend to the local tokens of a same region and their associated regional token. Note that the numbers denote the patch sizes at each stage of a model.

even worse in ViT as images are 2-D, suggesting a quadratic relationship between the number of tokens and image resolution. As a result, ViT indicates a quadruple complexity w.r.t image resolution. The highly compute- and memory-intensive self-attention makes it challenging to train vision transformer models at fine-grained patch sizes. It also significantly undermines the applications of these models to tasks such as object detection and semantic segmentation, which benefit from or require fine feature information computed from high-resolution images.

To address the aforementioned computational limitations of vision transformers, in this work, we develop a memory-friendly and efficient self-attention method for transformer models to reach their promising potential for vision applications. We propose a novel coarse-to-fine mechanism to compute self-attention in a hierarchical way. Specifically, our approach first divides the input image into a group of non-overlapping patches of large size (e.g.,  $28 \times 28$ ), on which *regional tokens* are computed via linear projection. Similarly, *local tokens* are created for each region using a smaller patch size (e.g.,  $4 \times 4$ ). We then use a standard transformer to process regional and local tokens separately. To enable communication between the two types of tokens, we first perform self-attention on regional tokens (*regional attention*) and then jointly attend to the local tokens of each region including their associated regional token (*local attention*). By doing so, regional tokens pass global contextual information to local tokens efficiently while being able to effectively learn from local tokens themselves. For clarity, we represent this two-stage attention mechanism as *Regional-to-Local Attention*, or *R2L attention* for short (see Fig. 1 for an illustration). Since both regional and local attention involve much fewer tokens, our R2L attention requires substantially less memory than regular global self-attention used in vision transformers. For example, in our default setting, the memory saving using R2L attention can be up to as much as 73%. We demonstrate the effectiveness of our approach on the image classification and several downstream vision tasks including object detection and action recognition.

To summarize, our key contributions in this work are as follows:

1. We propose a new vision transformer based on regional-to-local attention to learn both local and global features. Our proposed regional-to-local attention alleviates the overhead of standard global attention (too many tokens) and the weakness of pure local attention (no interaction between regions) used in existing vision transformers.
2. Our regional-to-local attention reduces the memory complexity significantly as compared to standard self-attention, leading to a savings in memory complexity by about  $\mathcal{O}(N/M^2)$ , where  $M$  is the window size of a region and  $N$  is the total number of tokens. This effectively allows us to train a more deep network for better performance while with comparable complexity.
3. Our models outperform or on par with several concurrent works on vision transformer that exploit pyramid structure for image classification. Experiments also demonstrate that our models work well on several downstream classification tasks, including object detection and action recognition.

Table 1: **Comparison to related works.** Most works use non-overlapped windows to group tokens, and then propose the corresponding methods to assure the information exchange among regions.

Methods	Structure	Attention Types	Windows of Local Attention	Handling Non-overlapped Regions	Global Tokens
ViT [13]	Isotropic	Global	N/A	N/A	N/A
PVT [43]	Pyramid	Global	N/A	N/A	N/A
Swin [30]	Pyramid	Local	Non-overlapped	Shifting the window	None
ViL [54]	Pyramid	Local + Global	Overlapped	N/A <sup>1</sup>	One learnable token
Twins [7]	Pyramid	Local + Global	Non-overlapped	GA	Subsampled from local tokens
Ours	Pyramid	Local + Regional	Non-overlapped	Regional-to-local attention	Regional tokens

GA: global attention. <sup>1</sup>: not applicable as ViL used overlapped windows.

## 2 Related Work

**CNNs with Attention.** Attention has been widely used for enhancing the features in the convolutional neural networks (CNNs), e.g., SENet [22] and CBAM [47] deploy channel and spatial attention for better feature representation. Various methods have been proposed that combine self-attention with CNNs [1, 36, 56, 34, 2, 21, 35, 44]. E.g., SAN [56] and SASA [34] attempts to replace all convolutional layers with local self-attention network. While these works show promising results, their complexity is relatively high due to the self-attention. On the other hand, BoTNet [36] replaces few convolutional layers with a slightly-modified self-attention to balance computation and accuracy. LambdaNet work [1] uses the approximated self-attention to reduce the overhead of self-attention and make the network efficient. Different from these works, our model utilizes regional-to-local attention to alleviate the workload of global self-attention by local attention while still keeping the global information via regional attention.

**Vision Transformer.** The vanilla vision transformer [13] (ViT) has recently achieved comparable results to CNN models when using a huge amount of data, e.g., JFT300M [37]. DeiT [40, 46] subsequently propose an efficient training scheme that allows vision transformer to work on par with CNN models while training only on ImageNet1K [11]. Despite promising performance of ViT, the architecture is directly borrowed from natural language processing, which might not be suitable for vision applications. Motivated by this, two main line of research works have been developed to improve ViT. One is to enhance different components of the vision transformer [51, 16, 41, 23] while still using isotropic structure (i.e., fixed token numbers and channel dimension) like ViT, e.g. while T2T-ViT [51] introduce an Tokens-to-Token (T2T) transformation to encode the important local structure for each token instead of the naive tokenization, CrossViT propose a dual-path architecture, each with different scales, to learn multi-scale feature. CaiT [41] propose a layer-scalar to assure training a deeper network for better performance and LV-ViT [23] modified how the model is trained when CutMix [52] augmentation is applied on ViT. Another parallel thread for improving vision transformer is in incorporating CNN-like pyramid structure into ViT [48, 43, 19, 54, 27, 15, 30, 7, 50, 6]. PVT [43] and PiT [19] introduce the pyramid structure of most CNN models into ViT, which makes them more suitable for objection detection as it can provide multi-scale features. LocalViT [27] and ConT [50] mix the convolutions with self-attention to encode the locality information. Swin [30], ViL [54] and Twins [7] limited the self-attention into a local region and then propose different methods to allow the interaction among each local region. Our model also utilizes pyramid structure and limits the self-attention in a local region; while we propose the regional-to-local attention to exchange the information among each region efficiently.

**Difference from PVT, Swin, ViL and Twins.** Table 1 summarizes the difference between our approach with the closely related works. PVT [43] uses pyramid structure but the scope of self-attention is still global. While ViL [54] limits self-attention into a local region, they adopt the *overlapped* windows as convolutions to process all the tokens. On the other hand, Swin [30], Twins [7] and ours adopt *non-overlapped* windows. While Swin [30] shift the position of windows alternatively in the consecutive transformer encoder to allow the interaction between regions, Twins [7] subsample local tokens as the global tokens, and then use the global tokens as the keys for self-attention to achieve the interaction between regions. By contrast, our proposed method utilizes a extra set of regional tokens with regional-to-local attention to perform self-attention on regional tokens only for the global information and then each regional token is sent to the associated local tokens to pass the global information to local tokens.

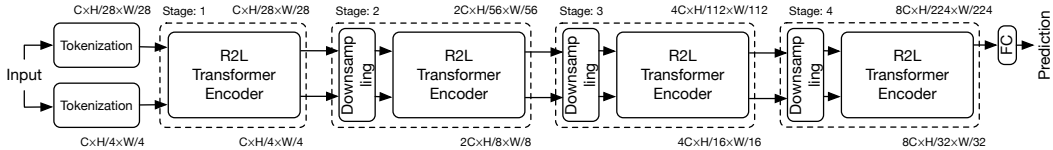


Figure 2: **Architecture of the proposed RegionViT.** There are mainly two paths in our proposed network where the upper path denotes regional tokens while the bottom path is for local tokens. The regional and local tokens are obtained based on two different tokenizations, and then they are passed through a sequence of regional-to-local (R2L) transformer encoders. After that, the regional tokens are used for the prediction. The Downsampling is a  $3 \times 3$  depthwise convolution which halves the spatial resolution and doubles the number of channels. The tensor shape of each stage is computed with the following settings: regional tokens take patch of  $28^2$ , local tokens take a patch of  $4^2$  and local window size is  $7^2$ .

### 3 Method

Our method is built on top of vision transformer [13], so we first present a brief background of ViT and then describe our method (RegionViT) on regional-to-local attention for vision transformers.

**Vision Transformer.** As opposed to CNN-based approaches for image classification, Vision transformer (ViT) [13] is a purely attention-based counterpart, borrowed from NLP. It consists of stacked transformer encoders, each of which contains a multihead self-attention (MSA) and a feed-forward network (FFN) with layer normalization and residual shortcut. To classify an image, ViT first splits it into patches of fixed size, e.g.  $16 \times 16$ , and then transforms them into tokens by linear projection. A class token is additionally prepended to the patch tokens to form the input sequence. Before the token are fed into transformer encoders, a learnable absolute positional embedding is added to each token to learn the position information. At the end of the network, the class token is used as the final feature representation for classification. Mathematically, ViT can be expressed as

$$\begin{aligned} \mathbf{x}_0 &= [\mathbf{x}_{cls} || \mathbf{x}_{patch}] + \mathbf{x}_{pos} \\ \mathbf{y}_k &= \mathbf{x}_{k-1} + \text{MSA}(\text{LN}(\mathbf{x}_{k-1})), \mathbf{x}_k = \mathbf{y}_k + \text{FFN}(\text{LN}(\mathbf{y}_k)), \end{aligned} \quad (1)$$

where  $\mathbf{x}_{cls} \in \mathbb{R}^{1 \times C}$  and  $\mathbf{x}_{patch} \in \mathbb{R}^{N \times C}$  are the class token and patch tokens respectively and  $\mathbf{x}_{pos} \in \mathbb{R}^{(1+N) \times C}$  is the position embedding.  $k$ ,  $N$  and  $C$  are the layer index, the number of patch tokens and dimension of the embedding, respectively.

While the vanilla ViT is ideally capable of learning global interaction among all the patch tokens, the memory complexity of self-attention become high when there are many tokens as the memory complexity is quadratically linear to the length of input sequence. Moreover, use of isotropic structure limits the capability of extending the vanilla ViT model to many vision applications that require high-resolution details, e.g. object detection. To address these issues, we propose regional-to-local attention for vision transformer, RegionViT for short.

**An Overview of Our Proposed Approach (RegionViT).** Figure 2 illustrates the architecture of the proposed vision transformer, which consists of two tokenization processes that convert an image into *regional* (upper path) and *local* tokens (lower path). Each tokenization is a convolution with different patch sizes, e.g., in Figure 2, the patch size of regional tokens is  $28^2$  while  $4^2$  is used for local tokens with dimensions projected to  $C$ , which means that one regional token covers  $7^2$  local tokens based on the spatial locality, leading to the window size of a local region to  $7^2$ . At stage 1, two set of tokens are passed through the proposed regional-to-local transformer encoders. However, for the later stages, to balance the computational load and to have feature maps at different resolution, we deploy a downsampling process to halve the spatial resolution while doubling the channel dimension like CNN on both regional and local tokens before going to the next stage. Finally, at the end of the network, we simply average the remaining regional tokens as the final embedding for the classification while the detection uses all local tokens at each stage since it provides more fine-grained location information. By having the pyramid structure, the ViT can generate multi-scale features and hence it could be easily extended to more vision applications, e.g., object detection, rather than image classification only. We explain the main components of regional-to-local transformer encoder in the next section.

**Regional-to-Local Transformer Encoder.** Figure 3 shows the proposed regional-to-local (R2L) transformer encoder which includes R2L attention and feed-forward network (FFN). Specifically,

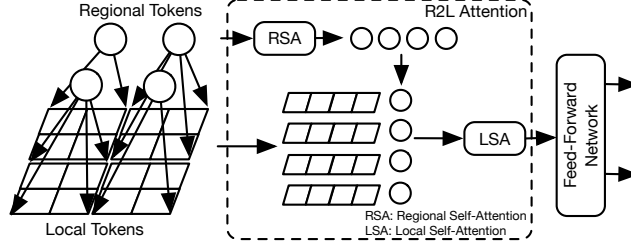


Figure 3: **Illustration of Regional-to-Local (R2L) Transformer Encoder.** All regional tokens are first passed through self-attention to exchange the information among regions and then regional-to-local MSA performs parallel self-attention where each takes one regional token and corresponding local tokens. This not only enhances the features by learning local context in a window but also learns the information from different regions due to the regional tokens. After that, all tokens are passed through the feed-forward network and split back to global and local tokens. Note that the all MSAs share the same weights, except for the layer normalization.

within R2L attention, the regional self-attention (RSA) first involves all regional tokens to learn the global information efficiently as the number of regional tokens is fewer and then local self-attention (LSA) takes the local tokens with the associated regional token to learn local feature while the involved regional token could provide global information at the same time. Both RSA and LSA are multihead self-attention (MSA) but with different input tokens. Finally, the FFN is applied to enhance the features. We also add layer normalization (LN) and residual shortcut as in standard transformer encoders. Mathematically, given the regional and local tokens,  $\mathbf{x}_r$  and  $\mathbf{x}_l$ , the R2L transformer encoder can be expressed as:

$$\begin{aligned} \mathbf{y}_r^l &= \mathbf{x}_r^{l-1} + \text{RSA}(\text{LN}(\mathbf{x}_r^{l-1})), \quad \mathbf{y}_{i,j}^l = [\mathbf{y}_{r_{i,j}}^l || \{\mathbf{x}_{l_{i,j,m,n}}^{l-1}\}_{m,n \in M}] \\ \mathbf{z}_{i,j}^l &= \mathbf{y}_{i,j}^l + \text{LSA}(\text{LN}(\mathbf{y}_{i,j}^l)), \quad \mathbf{x}_{i,j}^l = \mathbf{z}_{i,j}^l + \text{FFN}(\text{LN}(\mathbf{z}_{i,j}^l)) \end{aligned} \quad (2)$$

where  $l$  is the layer index,  $i, j$  are the spatial index with respect to regional tokens while  $m, n$  the index of local token in the window size  $M^2$ .

The RSA exchanges information among all tokens, which covers the context of whole image; while the LSA combines the features among the tokens belonging to the spatial region, including both regional and local tokens. Since the regions are divided by non-overlapped windows, the RSA is also designed to exchange the information among regions where the LSA takes one regional token and then combines with the local tokens in the same region. In such case, all local tokens are still capable of getting global information while being more focus on local neighbors. It is worth to note that the weights are shared between RSA and LSA except for the layer normalization; therefore, the number of parameters won't increase significantly when comparing to the standard transformer encoder. With these two attentions, the R2L can effectively and efficiently exchange the information among all regional and local tokens. In particular, the self-attention on regional tokens aim to extract high-level information and act as a bridge to pass information of local tokens from one region to other regions. On the other hand, the R2L attention focus on local contextual information with one regional token.

Moreover, the R2L transformer encoder can further reduce the memory complexity significantly. The memory complexity of self-attention usually consumes is  $\mathcal{O}(N^2)$ , where  $N$  is the number of local tokens. When a region contains  $M^2$  tokens, and there are  $N/(M^2)$  regions, the memory complexity is  $\mathcal{O}(N \times M^2)$ ; while the complexity from the attention on regional tokens is only  $\mathcal{O}((n_l/(M^2))^2)$ . Hence, the overall complexity becomes  $\mathcal{O}(NM^2 + (N/M^2)^2)$ . E.g., for a general case with  $N = 196$  and  $M = 7$ , the memory savings by our proposed method is  $\sim 73\%$ .

**Relative Position Bias.** Locality is an important clue for understanding the visual content; therefore, instead of adding absolute position embedding used by the regular ViT [13], we introduce the relative position bias into the attention map of R2L attention since relative position between patches (or pixels) are more important than the absolute position as the objects in the images can be places in an arbitrary way [34, 30]. Note that we only add this bias to the attention between local tokens and not the attention between regional token and local token. Specifically, for a given pair of local

tokens at the location,  $(x_m, y_m), (x_n, y_n)$ , the attention value  $a$  can be expressed as

$$a_{(x_m, y_m), (x_n, y_n)} = \text{softmax} \left( q_{(x_m, y_m)} k_{(x_n, y_n)}^T + b_{(x_m - x_n, y_m - y_n)} \right), \quad (3)$$

where  $b_{(x_m - x_n, y_m - y_n)}$  is taken from a learnable parameter  $B \in \mathbb{R}^{2M-1 \times 2M-1}$ , where  $M$  is the window size of a region. The first term  $q_{(x_m, y_m)} k_{(x_n, y_n)}^T$  is the attention value based on their content.

With relative position bias, our model does not require the absolute positional embedding as vanilla ViT since this relative position bias helps to encode the position information.

**Downsampling.** The spatial and channel dimension are changed along different stages of our network by simply applying  $3 \times 3$  depth-wise convolution with stride 2 for halving the resolution and doubling the channel dimension for both regional and local tokens (weights are shared) [19]. We also test with regular convolutions but it does not improve the accuracy with increase FLOPs and parameters.

**Regional Tokens.** The original ViT follows the original BERT to have a class token for classification; however, we can also consider that classification token is the abstract representation of an image. Therefore, we can design the regional tokens with the similar manner that having a set of class tokens as the regional tokens and each one for one region. Our results shown later in experiments show that using a set of learnable class tokens as regional tokens can result in good performance as it restricts the network to be only operate under the fixed resolution because the number of regional tokens are fixed. However, it is not easy to extend this to different vision tasks where image resolution is varied. Therefore, we adopt a simple flexible approach to generate regional tokens, by using linear projection with larger patch sizes. In this way, the number of regional tokens can adopt to different window size and the results are still competitive to the learnable one (see Table 8).

**Input Tokenization.** The tokenization can be implemented by using a  $4 \times 4$  convolution with channel size  $C$  and stride 4 (i.e. non-overlapped). However, as pointed out by prior works like T2T [51], CrossViT [5], and PiT [19], using a stronger but still simple subnetwork for the tokenization could further improve the performance, especially for the smaller models. Thus, we adopt one convolutional layer with overlapped kernel and identical stride when generating local tokens, e.g.  $8 \times 8$  as the kernel size. We found that for the smaller models, using few extra convolutions can boost the accuracy while the improvement is diminished when using deep transformers, which is consistent with the observation in the ViT [13]. Thus, we use 3 convolutional layers for the smaller models while only use 1 for the larger models (see Table 2 for details).

## 4 Experiments

In this section, we conduct extensive experiments to show that our RegionViT outperforms many competing approaches on image classification, object detection and action recognition. Table 2 summarizes the different RegionViT models with different width, depths and window sizes.

Table 2: Model architectures of RegionViT. For all networks, the dimension per head is 32 and the expanding ratio  $r$  in FFN is 4. The patch size of local tokens is always 4 while the patch size of regional tokens is  $4 \times M$ .

Model	Tokenization		Window size ( $M$ )	Dimension ( $C$ )	# of Encoders at each stage
	Local	Regional			
RegionViT-Ti	3-conv	linear	7	{64, 128, 256, 512}	{2, 2, 8, 2}
RegionViT-S	3-conv	linear	7	{96, 192, 384, 768}	{2, 2, 8, 2}
RegionViT-M	1-conv	linear	7	{96, 192, 384, 768}	{2, 2, 14, 2}
RegionViT-B	1-conv	linear	7	{128, 256, 512, 1024}	{2, 2, 14, 2}
RegionViT-Ti+	3-conv	linear	14	{64, 128, 256, 512}	{2, 2, 8, 2}
RegionViT-S+	3-conv	linear	14	{96, 192, 384, 768}	{2, 2, 8, 2}
RegionViT-M+	1-conv	linear	14	{96, 192, 384, 768}	{2, 2, 14, 2}
RegionViT-B+	1-conv	linear	14	{128, 256, 512, 1024}	{2, 2, 14, 2}

1-conv: Conv(k=8, s=4, p=3). 3-conv: Conv(k=3, s=2, p=1)  $\rightarrow$  Conv(k=3, s=2, p=1)  $\rightarrow$  Conv(k=3, s=1, p=1), LayerNorm and GeLU are added between Conv.

Table 3: Comparisons with recent pyramid-like structure ViT models on ImageNet1K. The bold number indicates the best number within the section.

Model	Params (M)	FLOPs (G)	Acc. (%)	Model	Params (M)	FLOPs (G)	Acc. (%)
PiT-XS [19]	10.6	1.4	78.1	ConT-M [50]	39.6	6.4	81.8
ConT-S [50]	10.1	1.5	76.5	Twins-PCPVT-B [7]	43.8	6.4	82.7
PVT-T [43]	13.2	1.9	75.1	PVT-M [43]	44.2	6.7	81.2
ConViT-Ti+ [10]	10.0	2.0	76.7	CvT-21 [48]	32.0	7.1	82.5
Twins-SVT-S [7]	24.0	2.8	<b>81.7</b>	Twins-SVT-B [7]	56	8.3	83.2
PiT-S [19]	23.5	2.9	80.9	ViL-M [54]	39.7	8.7	83.3
ConT-M [50]	19.2	3.1	80.2	Swin-S [30]	50.0	8.7	83.0
Twins-PCPVT-S [7]	24.1	3.7	81.2	PVT-L [43]	61.4	9.8	81.7
PVT-S [43]	24.5	3.8	79.8	ConViT-S+ [10]	48.0	10.0	82.2
RegionViT-Ti	13.8	2.4	80.4	NesT-S [55]	38.0	10.4	83.3
RegionViT-Ti+	14.3	2.7	81.5	RegionViT-M	41.2	7.4	83.1
DeiT-S [40]	22.1	4.6	79.9	RegionViT-M+	42.0	7.9	<b>83.4</b>
CvT-13 [48]	20.0	4.5	81.6	DeiT-B [40]	86.6	17.6	81.8
Swin-T [30]	29.0	4.5	81.3	PiB [19]	73.8	12.5	82.0
LocalViT-S [27]	22.4	4.6	80.8	ViL-B [54]	55.7	13.4	83.2
ViL-S [54]	24.6	4.9	82.0	Twins-SVT-L [7]	99.2	14.8	83.7
Visformer-S [6]	40.2	4.9	82.3	Swin-B [30]	88.0	15.4	83.3
ConViT-S [10]	27.0	5.4	81.3	ConViT-B [10]	86.0	17.0	82.4
NesT-S [55]	17.0	5.8	81.5	NesT-B [55]	68.0	17.9	<b>83.8</b>
RegionViT-S	30.6	5.3	82.5	RegionViT-B	72.7	13.0	83.3
RegionViT-S+	31.3	5.7	<b>83.2</b>	RegionViT-B+	73.8	13.6	<b>83.8</b>

#### 4.1 Image Classification

**Datasets.** We use ImageNet1K [11] (IN1K) and ImageNet21K [11] (IN21K) to validate our method. While ImageNet1K dataset contains 1.28 million training images and 50,000 validation images over 1,000 classes, the ImageNet21K is a large-scale dataset that consists of around 14 million images over 21,841 classes. We use all images for training and then finetune the model on ImageNet1K. On the other hand, we also perform the transfer learning from ImageNet1K to five downstream datasets (CIFAR10 [26], CIFAR100 [26], IIPets [33], StanfordCars [25] and ChestXRy8 [45]).

**Training and Evaluation.** We follow DeiT [40] to train our models on ImageNet1K [11] except that we use batch size 4,096 with base learning rate 0.004 and the warm-up epochs is 50. We adopt the AdamW [32] optimizer with cosine learning rate scheduler [31]. We apply Mixup [53], CutMix [52], RandomErasing [57], label smoothing [38], RandAugment [9] and instance repetition [20]. During training, we random cropped a  $224 \times 224$  region and take a  $224 \times 224$  center crop after resizing the shorter side to 256 for evaluation. We used the similar setting for ImageNet21K and transfer learning, and more details can be found in the supplementary material (ref. Section A.1).

**Results on ImageNet1K.** Table 3 shows the results on ImageNet1K where the methods listed all adopt CNN-like pyramid structure into the ViT and are all very recent and concurrent works. For the smaller models (Ti, S), RegionViT achieves better trade-off between accuracy and complexity (parameters or FLOPs); on the other hand, for the larger models (M and B), it obtains better accuracy while having fewer FLOPs and parameters. The efficiency of RegionViT comes from the proposed R2L attention, and hence with such efficiency, it enables the network to be wide and deep for the better accuracy with comparable complexity.

**Results on ImageNet21K.** Table 4 compares the ViT variants that use ImageNet21K for pretraining and then finetune on ImageNet1K with  $384 \times 384$  resolution. Overall, our models achieve good tradeoff between accuracy and model complexity. CvT-W24 [48] obtains best accuracy but it needs  $4 \times$  more parameters and FLOPs than RegionViT-B+. Moreover, RegionViT-B+ achieves same accuracy to Swin-L [30] with half parameters and FLOPs.

Table 4: IN1K results with IN21K.

Model	Params (M)	FLOPs (G)	Acc. (%)
CvT-21 [48]	32.0	25	84.9
ViL-M [54]	39.7	28.4	85.6
Swin-B [30]	88.0	47.0	<b>86.0</b>
RegionViT-M	41.7	19.8	85.4
RegionViT-B	72.7	39.2	<b>86.0</b>
ViL-B [54]	55.7	43.7	86.0
Swin-L [30]	197.0	103.9	86.4
CvT-W24 [30]	277	193.2	<b>87.7</b>
RegionViT-B+	76.5	42.6	86.5

#### Results on Transfer Learning.

Table 5 shows the transfer learning results on five image classification tasks with ImageNet1K pretrained weights. When transferring to the downstream task that mostly contains natural images, the performance of different models are similar. Nonetheless, our model outperforms DeiT [40] by 2~3% on ChestXRy8 [45], which has larger domain gap from ImageNet1K than other four datasets. We think this is because

Table 5: Transfer learning on downstream tasks.

	CIFAR10 [26]	CIFAR100 [26]	Pet [33]	StanfordCars [25]	ChestXRy8 [45]
DeiT-S [40]	99.1	90.9	94.9	91.5	55.4
DeiT-B [40]	99.1	90.8	94.4	91.7	55.8
RegionViT-S	98.9	90.0	95.3	92.8	57.8
RegionViT-M	99.0	90.8	95.5	91.9	58.3

Table 6: Object detection performance on the COCO val2017 with  $1\times$  schedule. The bold number indicates the best number within the section, and for MaskRCNN, both  $AP^b$  and  $AP^m$  are annotated.

Backbone	Params (M)	FLOPs (G)	RetinaNet							MaskRCNN						
			$AP$	$AP_{50}$	$AP_{75}$	$AP_s$	$AP_M$	$AP_L$	Params (M)	FLOPs (G)	$AP^b$	$AP_{50}^b$	$AP_{75}^b$	$AP^m$	$AP_{50}^m$	$AP_{75}^m$
ResNet50	37.7	234	36.3	55.3	38.6	19.3	40.0	48.8	44.2	260.0	38.0	58.6	41.4	34.4	55.1	36.7
ConT-M [50]	27.0	217.2	39.3	59.3	41.8	23.1	43.1	51.9	—	—	40.5	—	—	38.1	—	—
PVT-S [43]	34.2	—	40.4	61.3	43.0	25.0	42.9	55.7	44.1	—	40.4	62.9	43.8	37.8	60.1	40.3
ViL-S [54]	35.7	252.2	41.6	62.5	44.1	24.9	44.6	56.2	45.0	174.3	41.8	64.1	45.1	38.5	61.1	41.4
Swin-T [30]	38.5	245	41.5	62.1	44.2	25.1	44.9	55.5	47.8	264	42.2	64.6	46.2	39.1	61.6	42.0
Twins-SVT-S (w/ PEG) [7]	34.3	209	43.0	64.2	46.3	28.0	46.4	57.5	44.0	228	43.5	66.0	47.3	40.3	63.2	43.4
RegionViT-S	40.8	192.6	42.2	64.1	45.1	27.5	45.4	55.3	50.1	171.3	42.5	65.8	46.1	39.5	62.8	42.2
RegionViT-S+	41.5	204.2	43.1	64.8	46.2	29.6	46.6	56.1	50.9	182.9	43.5	66.9	47.5	40.4	63.7	43.4
RegionViT-S+ w/ PEG	41.6	204.3	<b>43.9</b>	65.5	47.3	28.5	47.3	57.9	50.9	183.0	<b>44.2</b>	67.3	48.2	<b>40.8</b>	64.1	44.0
ResNet101	56.7	315	38.5	57.8	41.2	21.4	42.6	51.1	63.2	336	40.4	61.1	44.2	36.4	57.7	38.8
ResNeXt101-32x4d	56.4	319.1	39.9	59.6	42.7	22.3	44.2	52.5	62.8	340	41.9	62.5	45.9	37.5	59.4	40.2
PVT-M [43]	53.9	—	41.9	63.1	44.3	25.0	44.9	57.6	63.9	—	42.0	64.4	45.6	39.0	61.6	42.1
ViL-M [54]	50.8	338.9	42.9	64.0	45.4	27.0	46.1	57.2	60.1	261.1	43.4	65.9	47.0	39.7	62.8	42.1
Swin-S [30]	59.8	335	44.5	65.7	47.5	27.4	48.0	59.9	69.1	354	44.8	66.6	48.9	40.9	63.4	44.2
Twins-SVT-B (w/ PEG) [7]	67.0	322	<b>45.3</b>	66.7	48.1	28.5	48.9	60.6	76.3	340	45.2	67.6	49.3	41.5	64.5	44.8
RegionViT-B	83.4	308.9	43.3	65.2	46.4	29.2	46.4	57.0	92.2	287.9	43.5	66.7	47.4	40.1	63.4	43.0
RegionViT-B+	84.4	328.1	44.2	66.2	47.1	29.2	47.5	58.6	93.2	307.1	44.5	67.6	48.7	41.0	64.4	43.9
RegionViT-B+ w/ PEG	84.5	328.2	44.6	66.4	47.6	29.6	47.6	59.0	93.2	307.2	<b>45.4</b>	68.4	49.6	<b>41.6</b>	65.2	44.8
ResNeXt101-64x4d	95.5	473	41.0	60.9	44.0	23.9	45.2	54.0	101.9	493	42.8	63.8	47.3	38.4	60.6	41.3
PVT-L [43]	71.1	345	42.6	63.7	45.4	25.8	46.0	58.4	81.0	364	42.9	65.0	46.6	39.5	61.9	42.5
ViL-B [54]	66.7	443.0	44.3	65.5	47.1	28.9	47.9	58.3	76.1	365.1	45.1	67.2	49.3	41.0	64.3	44.2
Swin-B [30]	98.4	477	44.7	65.9	49.2	—	—	—	107.2	496	45.5	—	—	41.3	—	—
Twins-SVT-L (w/ PEG) [7]	110.9	455	45.7	67.1	49.2	—	—	—	119.7	474	45.9	—	—	41.6	—	—
RegionViT-B+ w/ PEG†	84.5	506.4	<b>46.1</b>	68.0	49.5	30.5	49.9	60.1	93.2	464.4	<b>46.3</b>	69.1	51.2	<b>42.4</b>	66.2	45.6

The reported results of Swin [30] are from Twins [7] as the original paper does not include results with ImageNet1K weights. †: input resolution is  $896\times 1344$ .

the hierarchical feature models could provide better generalization for larger domain gap compared to DeiT [40] which uses isotropic spatial resolution throughout the whole network.

## 4.2 Object Detection

**Dataset.** We use MS COCO 2017 [29] to validate our models. COCO 2017 dataset contains 118K images for training and 5K images for validation across 80 categories.

**Training and Evaluation.** We adopt RetinaNet [28] and MaskRCNN [17] as our detection framework where simply replace the backbone with RegionViT, and then output the local tokens at each stages as multi-scale features for the detector. The regional tokens are not used in the detection. Before sending the features to the detector framework, we add new layer normalization layers to normalize the features. We use RegionViT-S and RegionViT-B as the backbone and the weights are initialized from ImageNet1K pretraining. The shorter side and longer side of the input image is resized the shorter and longer side of an image to 672 and 1,120, respectively. We train our models based on the settings in  $1\times$  schedule in Detectron2 [49], and more details can be found in supplementary material (ref. Section A.1).

**Results.** Table 6 compares RegionViT with SOTA transformer-based methods. For the smaller models, RegionViT-S and RegionViT-S+ achieve similar accuracy while being moderately efficient in terms of FLOPs. We find that the position encoding generator (PEG) in [8] could help the detection accuracy substantially, so we also provide the results with PEG, which are also used in Twins [7]. For the middle size models, RegionViT-B and RegionViT-B+ are slightly worse than Twins but still being more efficient. To compare the large models under similar FLOPs (RegionViT-B+ w/ PEG†), we further train our model with the similar resolution used by other works, and observe that our models outperform all others while being more parameter efficient (models marked with † in Table 6).

## 4.3 Action Recognition

**Datasets.** We validate our approach on Kinetics400 (K400) [24] and Something-Something V2 (SSV2) [14]. K400 has 240k training videos and 20k validation videos over 400 classes; while SSV2 contains 169k videos for training and 24k video for validation across 174 classes.

**Training and Evaluation.** We adopt the divided-space-time attention in TimeSformer [3] as the temporal modeling to perform action recognition experiments. More specifically, we plugin the temporal attention before every R2L transformer encoder and finetune the model pretrained with ImageNet1K (instead of ImageNet21K). We trained models with 8 frames with spatial size  $224\times 224$ , i.e. input is  $8\times 224\times 224$ . During evaluation, we take  $3\times 8\times 224\times 224$  spatial crops and then ensemble the predictions as the final prediction for the input video. More training details could be found in A.1



**Results.** Table 7 shows that with RegionViT as the backbone, the model can be much more efficient with competitive accuracy to TimeSformer [3], which uses vanilla ViT as the backbone. RegionViT-M could reduce more than 50% FLOPs and parameters than the TimeSformer. This not only shows the importance of spatial modeling in the action recognition but also validate that our proposed model can also be extended for efficient video action recognition.

Table 7: Performance on Action Recognition.

Model	FLOPs* (G)	Params (M)	K400 Acc. (%)	SSV2 Acc. (%)
TimeSformer [3]	197	121.4	75.8	59.5
TimeSformer† [3]	197	121.4	77.1	59.2
RegionViT-S	59.4	42.9	76.6	59.7
RegionViT-M	83.1	57.5	<b>77.6</b>	<b>59.8</b>

\*: FLOPs of single crop, †: retrained with the same setting.

#### 4.4 Ablation Study

We perform the following experiments to verify the effectiveness of different components in RegionViT. First, we validate the importance of regional tokens on image classification and object detection, and then evaluate different downsamplings and positional embedding on image classification.

**Regional Tokens.** Table 8 shows three different ways for regional tokens, including none, learnable and computed regional tokens. For image classification, the computed regional tokens provides around 0.5% improvement over no regional tokens with negligible overhead in both computations and parameters. Note that the learnable regional token implies that the network can only be operated at fixed input resolution while there is no such restriction when using computed regional tokens. Moreover, with the regional tokens, the performance of object detection is clearly improved even though regional tokens are not passed to the detector. This is because the image size for object detection is much larger such that the model needs to model the context for longer range, which can not be done by local attention only.

Table 8: Different regional tokens.

Regional Tokens	ImageNet1K Acc. (%)	MS COCO	
		MaskRCNN (AP <sup>b</sup> /AP <sup>m</sup> )	RetinaNet (AP <sup>b</sup> )
None	82.2	40.5/37.8	40.7
Learnable	82.7	N/A	N/A
Computed	82.6	42.2/39.0	41.7

RegionViT-S is used.

**Downsampling.** Table 9 shows different approaches for downsampling the patches.  $3 \times 3$  kernel size achieves better results than  $2 \times 2$  convolution, because the kernel is non-overlapped with  $2 \times 2$  convolution, which limits the interaction among local tokens. Moreover, using regular convolution does not improve the performance but increases computations and parameters. Thus, we use  $3 \times 3$  depthwise convolution for downsampling.

Table 9: Different downsampling approaches.

Downsampling	Params	FLOPs (G)	IN1K Acc. (%)
$2 \times 2$ convolution	32.1	5.5	82.3
$3 \times 3$ convolution	34.1	5.7	82.5
$3 \times 3$ depth-wise conv.	30.6	5.3	82.6

**Position information.** Table 10 compares performance of different combinations of absolute position embedding and relative position bias. The models with relative position bias achieve better accuracy with similar FLOPs and parameters. Even though the model with absolute position embedding could slightly improve the performance, it limits the model to run at fixed resolution, which is not suitable for vision tasks where image size could be varied. Thus, we only adopt the relative position bias in our models.

Table 10: Absolution position embedding and relative position bias.

Abs. pos.	Rel. pos.	Params (M)	FLOPs (G)	IN1K Acc. (%)
N	N	30.6	5.3	82.4
Y	N	30.9	5.3	82.2
Y	Y	30.9	5.3	82.7
N	Y	30.6	5.3	82.6

## 5 Conclusion

In this paper, we propose a new ViT architecture that exploits the pyramid structure used in most of CNNs to provide multi-scale features and hence, the models can be more easily extended to different vision applications, like object detection. Moreover, the proposed regional-to-local attention relaxes the memory overhead of performing self-attention on the fine-grained image tokens by limiting the scope of attention but still keep the capability to explore global information. Extensive experiments on several standard benchmark datasets well demonstrate that our proposed models outperform or on par with many concurrent ViT variants on three vision applications, including image classification, object detection and action recognition.

## A Appendix

**Summary** This supplementary material contains the following additional details. First, we describe the training details on image classification including the hyperparameters (see Table 11), and then describe the parameters for object detection and action recognition separately. Finally, we briefly describe the computing resource used for this work.

### A.1 Additional Training Details

**Image Classification.** We follow DeiT [40] to train our models on ImageNet1K [11] except that we use batch size 4,096 with base learning rate 0.004 and the warm-up epochs is 50. We adopt the AdamW [32] optimizer with cosine learning rate scheduler [31]. We apply Mixup [53], CutMix [52], RandomErasing [57], label smoothing [38], RandAugment [9] and instance repetition [20]. During training, we randomly crop a  $224 \times 224$  region and take a  $224 \times 224$  center crop after resizing the shorter side to 256 for evaluation. While pretraining on ImageNet21K [11], we use similar settings with slight modifications. We train the model using 120 epochs with 5 epochs for warmup, weight-decay of 0.01 and base learning rate of 0.001. For transfer learning experiments, we finetune the ImageNet1K pretrained models with 1,000 epochs, batch size of 768, learning rate of 0.01, SGD optimizer, weight decay of 0.0001, and using the same data augmentation in training on ImageNet1K. During evaluation, we resize the shorter side of an image to 256 and then take a  $224 \times 224$  region at the center and report top-1 accuracy. For finetuning experiments from ImageNet21K, we finetune the models with higher resolution of  $384 \times 384$ , for 30 epochs with cosine learning rate scheduler, base linear rate of 0.002, weight-decay of  $1e-8$ . Moreover, as it is trained on larger resolution, we adjust the window size  $M$  to have the same number of regional tokens at the first stage, e.g., we change the window size to 12 for the the models trained at  $224 \times 224$  with window size 7. We adopt the bicubic interpolation to upsample the weights of tokenizations and relative position bias. During evaluation, we directly resize the shorter side to 384 and then take center  $384 \times 384$  crop.

**Object Detection.** We adopt RetinaNet [28] and MaskRCNN [17] as our detection framework where simply replace the backbone with RegionViT, and then output the local tokens at each stages as multi-scale features for the detector. The regional tokens are not used in the detection. Before sending the features to the detector framework, we add new layer normalization layers to normalize the features. We use RegionViT-S and RegionViT-B as the backbone and the weights are initialized from ImageNet1K pretraining. We train our models based on the settings in  $1 \times$  schedule in Detec-tron2 [49], i.e., the batch size is 16 and the learning rate is set to 0.0001 which drops  $10 \times$  at the 60,000-th and 80,000-th iteration. We use AdamW optimizer with weight-decay of 0.05, and resize the shorter and longer side of an image to 672 and 1,120, respectively. We also adopt the drop-path when finetuning on the detector, with a rate set to 0.2 for both RetinaNet and MaskRCNN.

**Action Recognition.** We adopt the divided-space-time attention in TimeSformer [3] as the tempo-ral modeling to perform action recognition experiments. More specifically, we plugin the temporal attention before every R2L transformer encoder and finetune the model pretrained with ImageNet1K (instead of ImageNet21K). We use the AdamW optimizer [32] with base linear rate of  $2e-4$  and weight-decay of 0.0001. We apply the same Mixup [53], CutMix [52] and drop path [39] in the image classification. For the input, we uniformly sample 8 frames from the whole video and the  $224 \times 224$  region is cropped after shorter side of images is resized to the range of 256 to 320, result-ing the size of the input video as  $8 \times 224 \times 224$ . During evaluation, we use the same way to sample frames but take 3  $224 \times 224$  spatial crops (top-left, center and bottom-right) after resizing the shorter side of image to 256, and then ensemble the predictions as the final prediction for the input video.

### A.2 Computing Resource

For image classification and action recognition, we trained our models with 32 NVIDIA Tesla V100 GPUs while 8 GPUs for object detection.

Table 11: **Details of training settings for image classification on ImageNet1K and ImageNet21K.**

	IN1K	IN21K	Finetune to IN1K@384 <sup>2</sup>	Transfer
Batch size	4,096	4,096	1,024	768
Epochs	300	120	30	1,000
Optimizer	AdamW	AdamW	AdamW	SGD
Weight Decay	0.05	0.01	1e-8	1e-4
Linear-rate Scheduler (Initial LR)	Cosine (0.004)	Cosine (0.001)	Cosine (0.0002)	Cosine (0.01)
Warmup Epochs	50	5	0	5
Warmup linear-rate Scheduler (Initial LR)	Linear (1e-6)			
Data Aug.	RandAugment (m=9, n=2)			
Mixup ( $\alpha$ )	0.8			
CutMix ( $\alpha$ )	1.0			
Random Erasing	0.25			0.0
Instance Repetition*	3			
Drop-path	0.1			0.0
Label Smoothing	0.1			

\*: disabled for RegionViT-Ti.

## References

- [1] Irwan Bello. Lambdanetworks: Modeling long-range interactions without attention. In *International Conference on Learning Representations*, 2021.
- [2] Irwan Bello, Barret Zoph, Ashish Vaswani, Jonathon Shlens, and Quoc V Le. Attention augmented convolutional networks. In *Proceedings of the IEEE/CVF International Conference on Computer Vision*, pages 3286–3295, 2019.
- [3] Gedas Bertasius, Heng Wang, and Lorenzo Torresani. Is Space-Time Attention All You Need for Video Understanding? *arXiv.org*, February 2021.
- [4] Andrew Brock, Soham De, Samuel L Smith, and Karen Simonyan. High-Performance Large-Scale Image Recognition Without Normalization. *arXiv*, 2021.
- [5] Chun-Fu Chen, Quanfu Fan, and Rameswar Panda. CrossViT: Cross-Attention Multi-Scale Vision Transformer for Image Classification. *arXiv.org*, March 2021.
- [6] Zhengsu Chen, Lingxi Xie, Jianwei Niu, Xuefeng Liu, Longhui Wei, and Qi Tian. Visformer: The Vision-friendly Transformer. *arXiv.org*, April 2021.
- [7] Xiangxiang Chu, Zhi Tian, Yuqing Wang, Bo Zhang, Haibing Ren, Xiaolin Wei, Huaxia Xia, and Chunhua Shen. Twins: Revisiting Spatial Attention Design in Vision Transformers. *arXiv.org*, April 2021.
- [8] Xiangxiang Chu, Zhi Tian, Bo Zhang, Xinlong Wang, Xiaolin Wei, Huaxia Xia, and Chunhua Shen. Conditional Positional Encodings for Vision Transformers. *arXiv*, 2021.
- [9] Ekin Dogus Cubuk, Barret Zoph, Jon Shlens, and Quoc Le. RandAugment: Practical Automated Data Augmentation with a Reduced Search Space. In H Larochelle, M Ranzato, R Hadsell, M F Balcan, and H Lin, editors, *Advances in Neural Information Processing Systems*, pages 18613–18624. Curran Associates, Inc., 2020.
- [10] Stéphane d’Ascoli, Hugo Touvron, Matthew Leavitt, Ari Morcos, Giulio Biroli, and Levent Sagun. ConViT: Improving Vision Transformers with Soft Convolutional Inductive Biases. *arXiv.org*, cs.CV, 03 2021.
- [11] Jia Deng, Wei Dong, Richard Socher, Li-Jia Li, Kai Li, and Li Fei-Fei. Imagenet: A large-scale hierarchical image database. In *2009 IEEE conference on computer vision and pattern recognition*, pages 248–255. Ieee, 2009.
- [12] Jacob Devlin, Ming-Wei Chang, Kenton Lee, and Kristina Toutanova. BERT: Pre-training of deep bidirectional transformers for language understanding. In *Proceedings of the 2019 Conference of the North American Chapter of the Association for Computational Linguistics: Human Language Technologies, Volume 1 (Long and Short Papers)*, pages 4171–4186, Minneapolis, Minnesota, June 2019. Association for Computational Linguistics.
- [13] Alexey Dosovitskiy, Lucas Beyer, Alexander Kolesnikov, Dirk Weissenborn, Xiaohua Zhai, Thomas Unterthiner, Mostafa Dehghani, Matthias Minderer, Georg Heigold, Sylvain Gelly, Jakob Uszkoreit, and Neil Houlsby. An image is worth 16x16 words: Transformers for image recognition at scale. In *International Conference on Learning Representations*, 2021.
- [14] Raghav Goyal, Samira Ebrahimi Kahou, Vincent Michalski, Joanna Materzynska, Susanne Westphal, Heuna Kim, Valentin Haenel, Ingo Fruend, Peter Yianilos, Moritz Mueller-Freitag, et al. The "something something" video database for learning and evaluating visual common sense. In *ICCV*, 2017.
- [15] Ben Graham, Alaeldin El-Nouby, Hugo Touvron, Pierre Stock, Armand Joulin, Hervé Jégou, and Matthijs Douze. LeViT: a Vision Transformer in ConvNet’s Clothing for Faster Inference. *arXiv.org*, April 2021.
- [16] Kai Han, An Xiao, Enhua Wu, Jianyuan Guo, Chunjing Xu, and Yunhe Wang. Transformer in transformer. *arXiv preprint arXiv:2103.00112*, 2021.
- [17] Kaiming He, Georgia Gkioxari, Piotr Dollar, and Ross Girshick. Mask r-cnn. In *Proceedings of the IEEE International Conference on Computer Vision (ICCV)*, Oct 2017.
- [18] Kaiming He, Xiangyu Zhang, Shaoqing Ren, and Jian Sun. Deep Residual Learning for Image Recognition. In *The IEEE Conference on Computer Vision and Pattern Recognition (CVPR)*, June 2016.
- [19] Byeongho Heo, Sangdoon Yun, Dongyoon Han, Sanghyuk Chun, Junsuk Choe, and Seong Joon Oh. Rethinking Spatial Dimensions of Vision Transformers. *arXiv.org*, March 2021.
- [20] Elad Hoffer, Tal Ben-Nun, Itay Hubara, Niv Giladi, Torsten Hoefler, and Daniel Soudry. Augment your batch: Improving generalization through instance repetition. In *Proceedings of the IEEE/CVF Conference on Computer Vision and Pattern Recognition (CVPR)*, June 2020.
- [21] Han Hu, Zheng Zhang, Zhenda Xie, and Stephen Lin. Local relation networks for image recognition. In *Proceedings of the IEEE/CVF International Conference on Computer Vision*, pages 3464–3473, 2019.

- [22] J. Hu, L. Shen, and G. Sun. Squeeze-and-excitation networks. In *2018 IEEE/CVF Conference on Computer Vision and Pattern Recognition*, pages 7132–7141, 2018.
- [23] Zihang Jiang, Qibin Hou, Li Yuan, Daquan Zhou, Xiaojie Jin, Anran Wang, and Jiashi Feng. Token Labeling: Training a 85.4% Top-1 Accuracy Vision Transformer with 56M Parameters on ImageNet. *arxiv.org*, 04 2021.
- [24] Will Kay, Joao Carreira, Karen Simonyan, Brian Zhang, Chloe Hillier, Sudheendra Vijayanarasimhan, Fabio Viola, Tim Green, Trevor Back, Paul Natsev, et al. The kinetics human action video dataset. *arXiv:1705.06950*, 2017.
- [25] Jonathan Krause, Michael Stark, Jia Deng, and Li Fei-Fei. 3d object representations for fine-grained categorization. In *4th International IEEE Workshop on 3D Representation and Recognition (3dRR-13)*, Sydney, Australia, 2013.
- [26] Alex Krizhevsky, Geoffrey Hinton, et al. Learning multiple layers of features from tiny images. 2009.
- [27] Yawei Li, Kai Zhang, Jiezhong Cao, Radu Timofte, and Luc Van Gool. LocalViT: Bringing Locality to Vision Transformers. *arXiv.org*, April 2021.
- [28] Tsung-Yi Lin, Priya Goyal, Ross Girshick, Kaiming He, and Piotr Dollar. Focal loss for dense object detection. In *Proceedings of the IEEE International Conference on Computer Vision (ICCV)*, Oct 2017.
- [29] Tsung-Yi Lin, Michael Maire, Serge Belongie, James Hays, Pietro Perona, Deva Ramanan, Piotr Dollár, and C Lawrence Zitnick. Microsoft COCO: Common Objects in Context. In David Fleet, Tomas Pajdla, Bernt Schiele, and Tinne Tuytelaars, editors, *Computer Vision – ECCV 2014: 13th European Conference, Zurich, Switzerland, September 6-12, 2014, Proceedings, Part V*, pages 740–755. Springer International Publishing, Cham, 2014.
- [30] Ze Liu, Yutong Lin, Yue Cao, Han Hu, Yixuan Wei, Zheng Zhang, Stephen Lin, and Baining Guo. Swin Transformer: Hierarchical Vision Transformer using Shifted Windows. *arXiv.org*, March 2021.
- [31] Ilya Loshchilov and Frank Hutter. Sgdr: Stochastic gradient descent with warm restarts. In *International Conference on Learning Representations*, 2017.
- [32] Ilya Loshchilov and Frank Hutter. Decoupled weight decay regularization. In *International Conference on Learning Representations*, 2019.
- [33] Omkar M. Parkhi, Andrea Vedaldi, Andrew Zisserman, and C. V. Jawahar. Cats and dogs. In *IEEE Conference on Computer Vision and Pattern Recognition*, 2012.
- [34] Prajit Ramachandran, Niki Parmar, Ashish Vaswani, Irwan Bello, Anselm Levskaya, and Jon Shlens. Stand-Alone Self-Attention in Vision Models. In H Wallach, H Larochelle, A Beygelzimer, F d Alch e Buc, E Fox, and R Garnett, editors, *Advances in Neural Information Processing Systems*. Curran Associates, Inc., 2019.
- [35] Prajit Ramachandran, Niki Parmar, Ashish Vaswani, Irwan Bello, Anselm Levskaya, and Jonathon Shlens. Stand-alone self-attention in vision models. *arXiv preprint arXiv:1906.05909*, 2019.
- [36] Aravind Srinivas, Tsung-Yi Lin, Niki Parmar, Jonathon Shlens, Pieter Abbeel, and Ashish Vaswani. Bottleneck transformers for visual recognition. *arXiv preprint arXiv:2101.11605*, 2021.
- [37] C. Sun, A. Shrivastava, S. Singh, and A. Gupta. Revisiting unreasonable effectiveness of data in deep learning era. In *2017 IEEE International Conference on Computer Vision (ICCV)*, pages 843–852, 2017.
- [38] Christian Szegedy, Vincent Vanhoucke, Sergey Ioffe, Jon Shlens, and Zbigniew Wojna. Rethinking the inception architecture for computer vision. In *Proceedings of the IEEE Conference on Computer Vision and Pattern Recognition (CVPR)*, June 2016.
- [39] Mingxing Tan and Quoc Le. EfficientNet: Rethinking Model Scaling for Convolutional Neural Networks. In Kamalika Chaudhuri and Ruslan Salakhutdinov, editors, *Proceedings of the 36th International Conference on Machine Learning*, pages 6105–6114, Long Beach, California, USA, June 2019. PMLR.
- [40] Hugo Touvron, Matthieu Cord, Matthijs Douze, Francisco Massa, Alexandre Sablayrolles, and Hervé Jégou. Training data-efficient image transformers & distillation through attention. *arXiv preprint arXiv:2012.12877*, 2020.
- [41] Hugo Touvron, Matthieu Cord, Alexandre Sablayrolles, Gabriel Synnaeve, and Hervé Jégou. Going deeper with Image Transformers. *arXiv.org*, cs.CV, 03 2021.
- [42] Ashish Vaswani, Noam Shazeer, Niki Parmar, Jakob Uszkoreit, Llion Jones, Aidan N Gomez, ukasz Kaiser, and Illia Polosukhin. Attention is All you Need. In I Guyon, U V Luxburg, S Bengio, H Wallach, R Fergus, S Vishwanathan, and R Garnett, editors, *Advances in Neural Information Processing Systems*. Curran Associates, Inc., 2017.
- [43] Wenhai Wang, Enze Xie, Xiang Li, Deng-Ping Fan, Kaitao Song, Ding Liang, Tong Lu, Ping Luo, and Ling Shao. Pyramid vision transformer: A versatile backbone for dense prediction without convolutions, 2021.

- [44] Xiaolong Wang, Ross Girshick, Abhinav Gupta, and Kaiming He. Non-local neural networks. In *Proceedings of the IEEE conference on computer vision and pattern recognition*, pages 7794–7803, 2018.
- [45] Xiaosong Wang, Yifan Peng, Le Lu, Zhiyong Lu, Mohammadhadi Bagheri, and Ronald M Summers. Chestx-ray8: Hospital-scale chest x-ray database and benchmarks on weakly-supervised classification and localization of common thorax diseases. In *Proceedings of the IEEE conference on computer vision and pattern recognition*, pages 2097–2106, 2017.
- [46] Ross Wightman. Pytorch image models. <https://github.com/rwightman/pytorch-image-models>, 2019.
- [47] Sanghyun Woo, Jongchan Park, Joon-Young Lee, and In So Kweon. Cbam: Convolutional block attention module. In *Proceedings of the European Conference on Computer Vision (ECCV)*, September 2018.
- [48] Haiping Wu, Bin Xiao, Noel Codella, Mengchen Liu, Xiyang Dai, Lu Yuan, and Lei Zhang. CvT: Introducing Convolutions to Vision Transformers. *arXiv.org*, March 2021.
- [49] Yuxin Wu, Alexander Kirillov, Francisco Massa, Wan-Yen Lo, and Ross Girshick. Detectron2. <https://github.com/facebookresearch/detectron2>, 2019.
- [50] Haotian Yan, Zhe Li, Weijian Li, Changhu Wang, Ming Wu, and Chuang Zhang. ConTNet: Why not use convolution and transformer at the same time? *arXiv.org*, April 2021.
- [51] Li Yuan, Yunpeng Chen, Tao Wang, Weihao Yu, Yujun Shi, Francis EH Tay, Jiashi Feng, and Shuicheng Yan. Tokens-to-token vit: Training vision transformers from scratch on imagenet, 2021.
- [52] Sangdoon Yun, Dongyoon Han, Seong Joon Oh, Sanghyuk Chun, Junsuk Choe, and Youngjoon Yoo. Cut-Mix: Regularization Strategy to Train Strong Classifiers With Localizable Features. In *Proceedings of the IEEE/CVF International Conference on Computer Vision (ICCV)*, October 2019.
- [53] Hongyi Zhang, Moustapha Cisse, Yann N. Dauphin, and David Lopez-Paz. mixup: Beyond empirical risk minimization. In *International Conference on Learning Representations*, 2018.
- [54] Pengchuan Zhang, Xiyang Dai, Jianwei Yang, Bin Xiao, Lu Yuan, Lei Zhang, and Jianfeng Gao. Multi-Scale Vision Longformer: A New Vision Transformer for High-Resolution Image Encoding. *arXiv.org*, March 2021.
- [55] Zizhao Zhang, Han Zhang, Long Zhao, Ting Chen, and Tomas Pfister. Aggregating Nested Transformers. *arXiv*, 2021.
- [56] Hengshuang Zhao, Jiaya Jia, and Vladlen Koltun. Exploring self-attention for image recognition. In *Proceedings of the IEEE/CVF Conference on Computer Vision and Pattern Recognition (CVPR)*, June 2020.
- [57] Zhun Zhong, Liang Zheng, Guoliang Kang, Shaozi Li, and Yi Yang. Random Erasing Data Augmentation. *Proceedings of the AAAI Conference on Artificial Intelligence*, 34(07):13001–13008, April 2020.